engineering proceedings

MDPI

Proceeding Paper

Insights and Implications: Unraveling Critical Factors in Resistance Spot Welding of Dissimilar Metals through SS 347 and DSS 2205 Welds †

Prabhakaran M. [1,2,*], Jeyasimman D. [1] and Varatharajulu M. [3]

[1] Department of Mechanical Engineering, Periyar Maniammai Institute of Science & Technology, Thanjavur 613 403, Tamil Nadu, India; jeyasimman76@gmail.com
[2] Department of Mechanical Engineering, Agnel Institute of Technology and Design, Assagao 403 507, Goa, India
[3] Department of Mechanical Engineering, Sri Krishna College of Technology, Kovaipudur 641 042, Tamil Nadu, India; rajulu_production@yahoo.co.in
* Correspondence: global.prabhakaran@gmail.com; Tel.: +91-99229-65256
† Presented at the International Conference on Recent Advances on Science and Engineering, Dubai, United Arab Emirates, 4–5 October 2023.

Abstract: This research focuses on analyzing the microstructural and mechanical characteristics of SS 347 and DSS 2205 stainless steel dissimilar welds. This is achieved by altering the weld parameters, welding current and heating cycle at three different levels each. In total, nine experimental trials were conducted and the welded sheets were applied to macrograph studies and a tensile shear test for analyzing the nugget quality and mechanical strength. The welded specimens were placed for observation under a scanning electron microscope (SEM) to observe the microstructure of the weldments. Specimen 9 was subjected to a microhardness test. The macrograph study revealed that the nugget size grows proportionally to the rise in the welding current and heating cycle. When the current exceeds 7.5 kA, the size of the nugget exceeds the threshold value of $4\sqrt{t}$, where 't' is the sheet metal thickness. The tensile shear test results clearly indicate that as the nugget size grows, the tensile force also rises. Sample 9 possesses a maximum tensile force of 18 kN and the mode of failure observed is influenced by the welding current and heating cycles. The failure mode of sample 9 was pulled out and the microhardness was maximum at the fusion zone with 320 HV.

Keywords: SS 347; DSS 2205; tensile shear test; dissimilar resistance spot welding; microhardness

check for updates

Citation: M., P.; D., J.; M., V. Insights and Implications: Unraveling Critical Factors in Resistance Spot Welding of Dissimilar Metals through SS 347 and DSS 2205 Welds. *Eng. Proc.* **2023**, *59*, 27. https://doi.org/10.3390/engproc2023059027

Academic Editors: Nithesh Naik, Rajiv Selvam, Pavan Hiremath, Suhas Kowshik CS and Ritesh Ramakrishna Bhat

Published: 12 December 2023

Copyright: © 2023 by the authors. Licensee MDPI, Basel, Switzerland. This article is an open access article distributed under the terms and conditions of the Creative Commons Attribution (CC BY) license (https://creativecommons.org/licenses/by/4.0/).

1. Introduction

Resistance spot welding (RSW) is a highly popular and widely used method for joining delicate sheet metals. Due to its versatility, it finds extensive application in various industries. Stainless steels are predominantly used for their anti-corrosive nature in harsh environments. The increasing requirements of the processing and fabrication industry have given rise to the need for dissimilar welding. Xu et al. [1] performed a lap shear test investigation on different types of body-in-white steel plates with and without coatings of varying thicknesses. The failure mechanisms were analyzed through microstructure, and a new parameter, namely standardized shear strength, was coined. Ghanbari et al. [2] investigated the fatigue behavior of the dissimilar RSW between dual-phase steel joints made using hybrid joints with the aid of adhesives. The results confirmed that the adhesives are beneficial in obtaining a better fatigue life and strength. Badkoobeh et al. [3] conducted RSW experiments on dual-phase steel sheets. They observed that a rise in silicon presence up to 1.51% by weight increases the fracture energy, and any further rise in silicon content results in a reduction in the fracture energy. Ling et al. [4] studied the LME cracking during the RSW. As a result of a hot tensile test, it was concluded that the risk of embrittlement cracking is higher in galvanized Q&P 980 steel as compared to low-carbon steel. In a typical

study carried out by Sivaraj et al. [5], similar joints of DP600 dual-phase steel were obtained using varying weld parameters. According to the tensile shear test, the welds' strength was found to upsurge with an ascent in welding current to a certain extent, beyond which it was degraded. Pouranvari et al. [6] identified that the extremely fast rate of cooling of the RSW joints highly influences the phase transformation of the fusion zone of duplex and austenitic stainless steels. Liu et al. [7] analyzed the phase transformations in the RSW of Q&P980 steel by categorizing the welded region into several zones. This paper aims toward the mechanical characterization of dissimilar RSW performed with duplex stainless steel (DSS) and austenitic stainless steel (ASS) sheets. The varying mechanical properties of these two metals and different phase structures make the welding between them challenging. In order to obtain a proper weld nugget and optimal weld strength, the weld parameters need to be evaluated through proper experimental design. The influence of the weld constraints on weld nugget formation, and its mechanical strength, is studied in detail through our experiments. The defect-free nuggets are more significant for obtaining structural integrity and better weld characteristics in terms of strength, corrosion resistance, and anti-leakage characteristics.

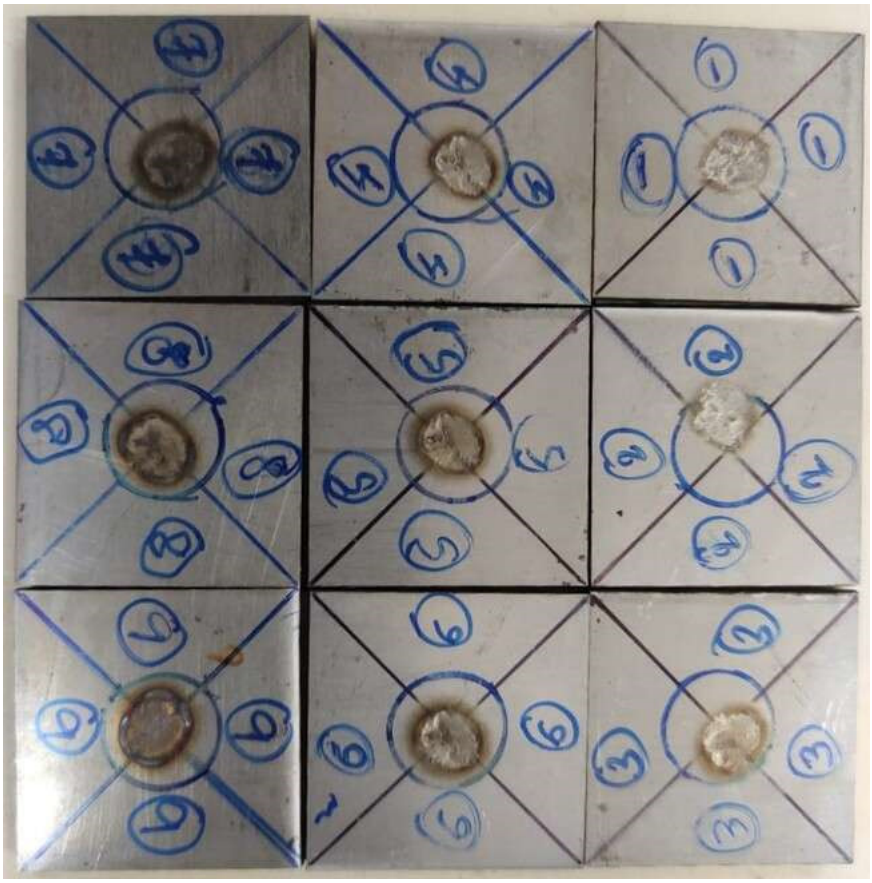
2. Materials and Methods

This research paper details the mechanical properties of the dissimilar RSW of AISI ASS347 and DSS2205, and the compositions of the stainless steels are as mentioned by Prabhakaran et al. [8]. ASS 347 is a niobium-stabilized grade of austenitic stainless steel [9,10]. DSS2205 is predominantly known for its anti-corrosive property and superior strength [11]. The chemical composition of the stated materials is provided in Table 1. The experimental design was conducted with three constant and two variable weld parameters. The welding current was varied at three levels, 6.5 kA, 7.5 kA, and 8.5 kA, and the electrode tip diameter was 10 mm. The heating time cycle was also varied at three levels, 10, 12, and 14 cycles. The squeezing time was 50 cycles, and the holding time was kept at 10 cycles with a total of 9 trials.

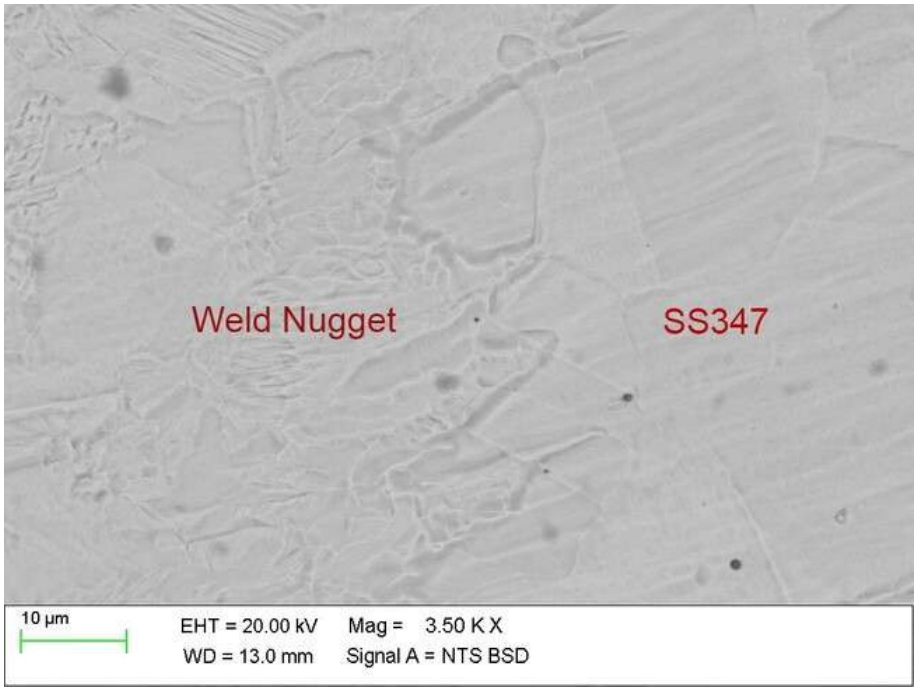
Table 1. Chemical composition of AISI 347 and DSS 2205.

Name of the element	C	Mn	Si	Cr	P	Ni	S	Nb	Fe
AISI 347 composition (%)	0.08	2	0.75	19	0.045	0.02	0.03	1	Rest
DSS 2205 composition (%)	0.02	0.82	0.36	22.3	0.03	5.46	0.01	-	Rest

The microprocessor-controlled Nash 815 V2 RSW machine, operated manually through a pedal, was utilized for conducting the RSW process. The welded specimens shown in Figure 1a were subjected to macrograph studies. The cut specimens were placed under a tensile shear test (TST) to evaluate their mechanical strength, and studied under a scanning electron microscope (SEM) to determine their microstructure and phase transformation.

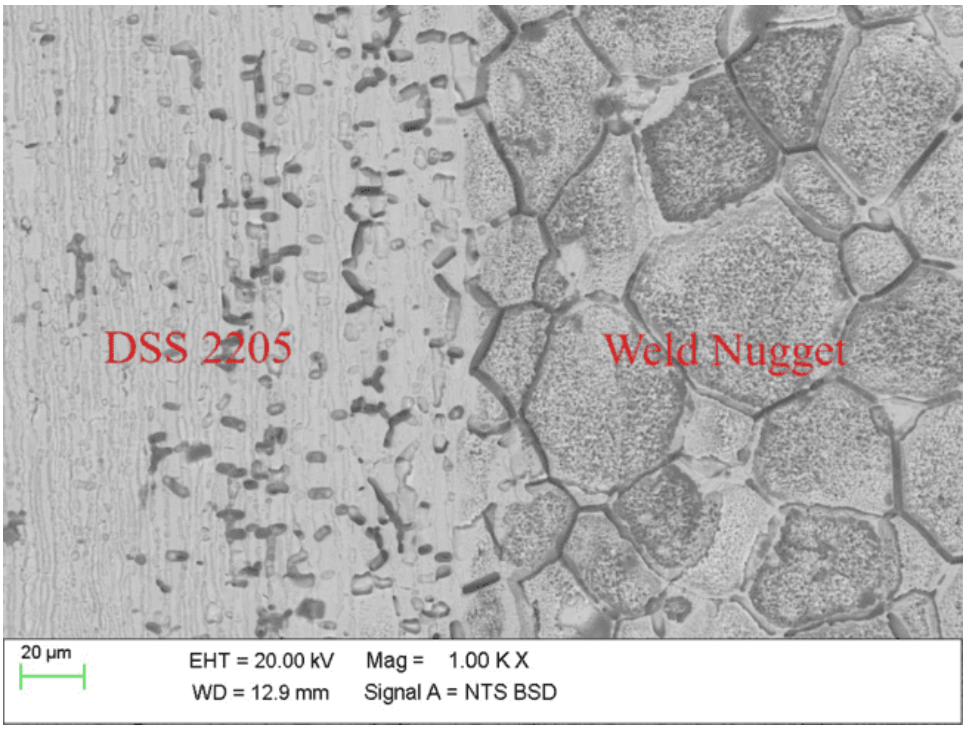


(**a**)



(**b**)

Figure 1. *Cont.*



(**c**)

Figure 1. (**a**) Welded specimens. (**b**) Interface of SS347 with weld nugget. (**c**) Interface of DSS2205 with weld nugget.

3. Results

Figure 2 shows the macrograph images of the specimens. The experimental design shown in Table 2 mentions the welding current and heat cycles corresponding to each sample. Hence, it can be observed that for each sample, the heating cycle and welding current keep on increasing. Figure 1b,c show the SEM images of the interface of AISI SS347 and DSS 2205 with the weld the nugget, respectively. The region between the SS347 and the weld nugget interface reveals a gradual transformation of the austenitic phase from the base metal region to a mixture of δ-ferritic and austenitic regions in the weld zone [12,13]. A similar transformation can be seen in Figure 1c where the ferritic structure in the DSS 2205 slowly fades away into the austenitic phase in the weld zone.

This transformation is highly affected by the weld parameters and is evident in the macrograph images. In samples 2, 3, 4, and 5, the nugget formation is not proper and contains void spaces in it. This represents insufficient heat supplied for weld pool formation. In spite of retentive heating cycles, a welding current up to 7.5 kA is not sufficient for proper weld nugget formation. On the other hand, upon the inspection of weld samples 6 to 9, the weld nugget is complete with no voids. Hence, a welding current of up to 8.5 kA is required for the chosen material and thickness.

The weld size is represented in terms of the length and thickness of the nugget and is directly proportional to the weld strength. Figure 3a shows the variation in the nugget length and thickness for all the welded specimens. Based on the analysis, it can be found that as the heating cycle and welding current are amplified, there is a corresponding augment in the magnitude of the weld nugget.

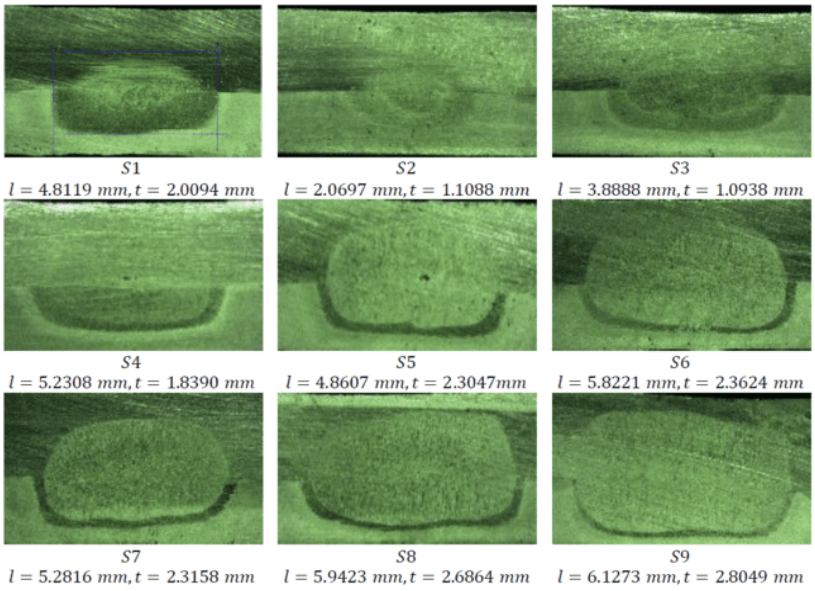
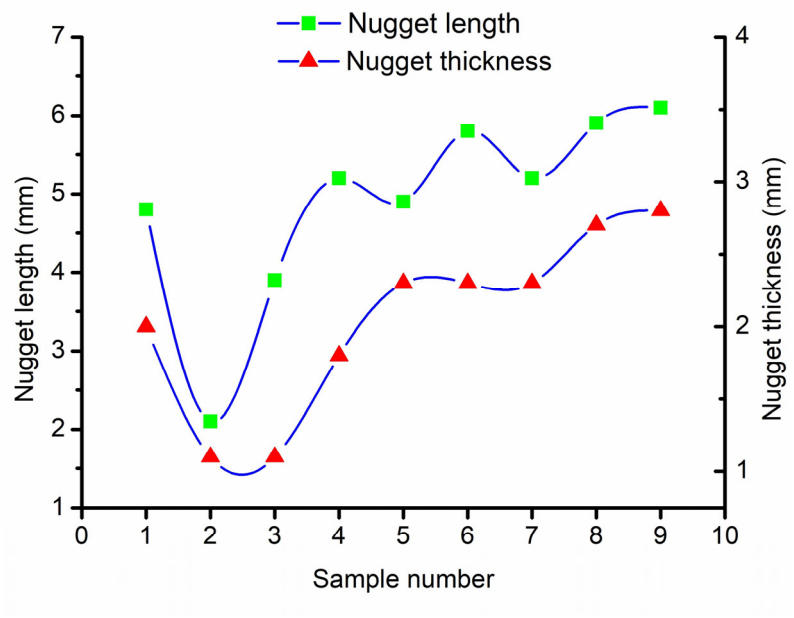


Figure 2. Macro morphology of the welded specimen.

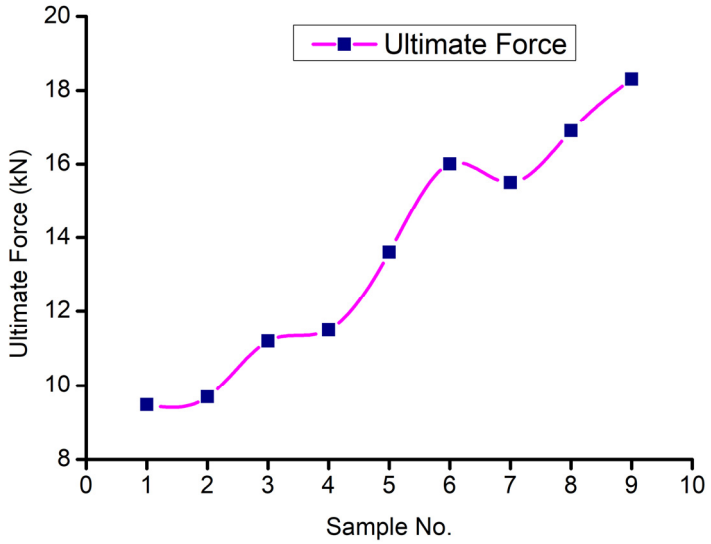
Table 2. Welded specimen in various parameters.

Trial No.	1	2	3	4	5	6	7	8	9
Welding Current (kA)	6.5	6.5	6.5	7.5	7.5	7.5	8.5	8.5	8.5
Heating time (cycles)	10	12	14	10	12	14	10	12	14

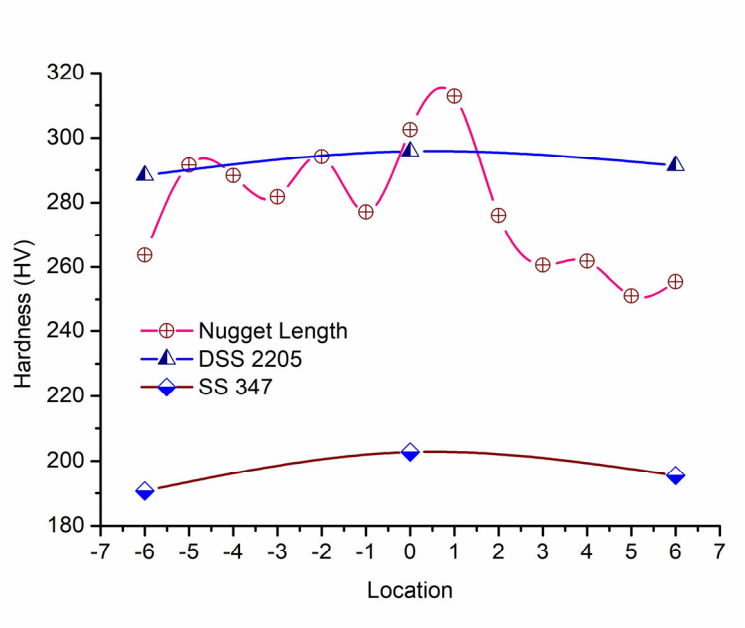


(**a**)

Figure 3. *Cont.*



(**b**)



(**c**)

Figure 3. (**a**) Nugget length and thickness. (**b**) Ultimate force. (**c**) Nugget hardness variation with respect to substrate hardness.

For the purpose of conducting a tensile shear test, a separate batch of nine samples was welded in the lap joint position, employing an identical experimental design. From Figure 3b, it can be easily understood that the strength of the weld rises with the ascent in heating value and current [14]. As stated in the previous section, a rise in the independents has resulted in a larger weld nugget, and from the TST results, the direct correlation of the weld size with the ultimate strength can be realized. A critical argument that cannot be overlooked is the minimum dimension of the weld nugget for the given material thickness. The minimum weld nugget dimension considered to be eligible as a proper weld is given by the relation $4\sqrt{t}$, where t is the sheet metal thickness [13,15]. For this research purpose, the base material thickness is chosen as 2 mm and hence the eligible weld nugget size would be 5.6 mm. In this regard, samples 6, 8, and 9 comply with the specified nugget size, and the macrograph studies also confirm that only these samples are defect-free and complete.

Thus, when evaluating the results of the macrograph studies with the TST results, the poor tensile strength of samples 1 to 5 can be attributed to the defects and smaller size of the fusion zone. Figure 3c displays the distribution of hardness in both the base metal and the fusion zone. The hardness values of the duplex stainless steel are found to be superior to the austenitic stainless steel [16]. The hardness at the fusion zone is found to be larger than that of the duplex steel due to the phase change [17]. The failure mode of samples 1 to 8 was interfacial failure, whereas sample 9 was in pull-out failure mode, which is attributed to the rise in hardness of the weld nugget with respect to the base metal [18–20]. This pull-out failure mode signifies that the weld nugget formation is proper and strong enough to hold the load applied, and the failure occurs only through the base metal region.

4. Conclusions

The investigation of RSW between AISI SS347 and DSS 2205 has yielded significant findings, as follows:

- Weld nugget size exhibits a direct correlation with weld current, with larger nuggets formed when using a higher current. However, it has been observed that nuggets formed with less than 7.5 kA welding current may contain defects.
- The ultimate tensile force of the welded specimens rises in proportion to the weld nugget dimension. Additionally, the presence of defects within the nugget affects both the maximum ultimate force and the failure mode exhibited by the specimens.
- During welding with 8.5 kA current and a 14-cycle heating time, the increase in hardness of the welded specimens has led to a pull-out failure mode [21].

These findings highlight the critical relationship between weld parameters, nugget characteristics, and the mechanical characteristics of dissimilar RSW joints between AISI SS347 and DSS 2205.

Author Contributions: Conceptualization and original draft preparation, P.M.; investigation, and review and editing, V.M.; formal analysis and supervision, J.D. All authors have read and agreed to the published version of the manuscript.

Funding: This research received no external funding.

Data Availability Statement: Data is unavailable due to ethical restrictions from other journals.

Conflicts of Interest: The authors declare no conflict of interest.

References

1. Xu, Z.; Xiao, A.; Jiang, S.; Mao, L.; Tian, H.; Yi, B.; Ling, H. Effect of plate thickness on mechanical properties and failure behaviors of resistance spot welded advanced high strength steels. *J. Manuf. Process.* **2023**, *95*, 392–404. [CrossRef]
2. Ghanbari, H.R.; Shariati, M.; Sanati, E.; Nejad, R.M. Effects of spot welded parameters on fatigue behavior of ferrite-martensite dual-phase steel and hybrid joints. *Eng. Fail. Anal.* **2022**, *134*, 106079. [CrossRef]
3. Badkoobeh, F.; Nouri, A.; Hassannejad, H.; Mostaan, H. Microstructure and mechanical properties of resistance spot welded dual-phase steels with various silicon contents. *Mater. Sci. Eng. A* **2020**, *790*, 139703. [CrossRef]
4. Ling, Z.; Wang, M.; Kong, L.; Chen, K. Towards an explanation of liquid metal embrittlement cracking in resistance spot welding of dissimilar steels. *Mater. Des.* **2020**, *195*, 109055. [CrossRef]
5. Sivaraj, P.; Seeman, M.; Kanagarajan, D.; Seetharaman, R. Influence of welding parameter on mechanical properties and microstructural features of resistance spot welded dual phase steel sheets joint. In *Materials Today: Proceedings*; Elsevier Ltd.: Amsterdam, The Netherlands, 2020; pp. 558–562. [CrossRef]
6. Pouranvari, M.; Alizadeh-Sh, M.; Marashi, S.P.H. Welding metallurgy of stainless steels during resistance spot welding part I: Fusion zone. *Sci. Technol. Weld. Join.* **2015**, *20*, 502–511. [CrossRef]
7. Liu, T.; Wang, H.; Yang, H.; Ke, C.; Zhou, L.; Zhao, H. Microstructure of resistance spot weld ultra high strength steel Q&P980. In *IOP Conference Series: Materials Science and Engineering*; Institute of Physics Publishing: Bristol, UK, 2019. [CrossRef]
8. Prabhakaran, M.; Duraisamy, J.; Shanmugam, N.S.; Kannan, A.R.; Varatharajalu, M. Weld Strength and Microstructure Analysis on Resistance Spot Welding of Austenitic AISI 347 Stainless Steel and Duplex AISI 2205 Stainless Steel. *Trans. Indian Inst. Met.* **2023**, *76*, 925–936. [CrossRef]
9. Kain, V. *Corrosion-Resistant Materials*; Elsevier Inc.: Amsterdam, The Netherlands, 2011. [CrossRef]
10. Kumar, M.S.; Gopi, S.; Sivashanmugam, N.; Sasikumar, A. A study on corrosion behavior of stainless steel dissimilar alloy weld joints (321 & 347). *Mater Today Proc.* **2021**, *46*, 9229–9231. [CrossRef]

11. García-García, V. Microstructural and mechanical analysis of double pass dissimilar welds of twinning induced plasticity steel to austenitic/duplex stainless steels. *Int. J. Press. Vessel. Pip.* **2022**, *198*, 104665. [CrossRef]
12. Dak, G.; Sirohi, S.; Pandey, C. Study on microstructure and mechanical behavior relationship for laser-welded dissimilar joint of P92 martensitic and 304L austenitic steel. *Int. J. Press. Vessel. Pip.* **2022**, *196*, 104629. [CrossRef]
13. Bhat, S.D.; Vijeesh, V.; Acharya, P.; Rao, M. Investigation of thin sheet stainless steel resistance spot welds: Effect of weld current on nugget failure and microstructure. *Mater. Today Proc.* **2021**, *35*, 361–365. [CrossRef]
14. Hassoni, S.M.; Barrak, O.S.; Ismail, M.I.; Hussein, S.K. Effect of Welding Parameters of Resistance Spot Welding on Mechanical Properties and Corrosion Resistance of 316L. *Mater. Res.* **2022**, *25*. [CrossRef]
15. Krishnan, V.; Ayyasamy, E.; Paramasivam, V. Influence of resistance spot welding process parameters on dissimilar austenitic and duplex stainless steel welded joints. *Proc. Inst. Mech. Eng. Part E* **2021**, *235*, 12–23. [CrossRef]
16. Kumar, A.; Panda, S.; Ghosh, G.K.; Patel, R.K. Numerical simulation of weld nugget in resistance spot welding process. *Mater. Today Proc.* **2019**, *27*, 2958–2963. [CrossRef]
17. Arabi, S.H.; Pouranvari, M.; Movahedi, M. Welding metallurgy of duplex stainless steel during resistance spot welding. *Weld. J.* **2017**, *96*, 307s–318s.
18. Sheikhi, M.; Jaderian, S.; Mazaheri, Y.; Pouranvari, M. Prediction of the failure mode of automotive steels resistance spot welds. *Sci. Technol. Weld. Join.* **2020**, *25*, 511–517. [CrossRef]
19. Onar, V. Mechanical and Microstructural Characterizations of Resistance Spot Welded Dissimilar TWIP/304L Stainless Steel. *Trans. Indian Inst. Met.* **2022**, *75*, 1731–1739. [CrossRef]
20. Sobhani, S.; Pouranvari, M. Duplex stainless steel/martensitic steel dissimilar resistance spot welding: Microstructure-properties relationships. *Weld. J.* **2019**, *98*, 263S–272S. [CrossRef]
21. Prabhakaran, M. Investigation of the failure mechanism of dissimilar resistance spot welding of steels. *Emerg. Mat. Res.* **2023**, *12*, 220–228. [CrossRef]

Disclaimer/Publisher's Note: The statements, opinions and data contained in all publications are solely those of the individual author(s) and contributor(s) and not of MDPI and/or the editor(s). MDPI and/or the editor(s) disclaim responsibility for any injury to people or property resulting from any ideas, methods, instructions or products referred to in the content.